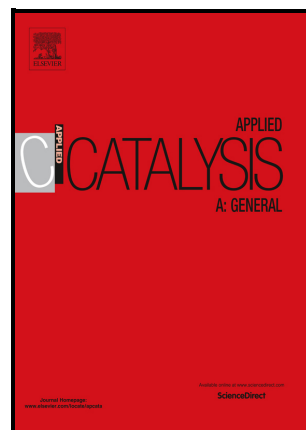


Production of a high molecular weight jet-fuel precursor from biomass derived furfural and 2-methylfuran using propyl sulfonic SBA-15 catalysts

M.S. Zanuttini, L.G. Tonutti, C.A. Neyertz, C. Ferretti, B.S. Sanchez, B.O. Dalla Costa, C.A. Querini



PII: S0926-860X(23)00363-0

DOI: <https://doi.org/10.1016/j.apcata.2023.119383>

Reference: APCATA119383

To appear in: *Applied Catalysis A, General*

Received date: 22 May 2023

Revised date: 17 August 2023

Accepted date: 18 August 2023

Please cite this article as: M.S. Zanuttini, L.G. Tonutti, C.A. Neyertz, C. Ferretti, B.S. Sanchez, B.O. Dalla Costa and C.A. Querini, Production of a high molecular weight jet-fuel precursor from biomass derived furfural and 2-methylfuran using propyl sulfonic SBA-15 catalysts, *Applied Catalysis A, General*, (2023) doi:<https://doi.org/10.1016/j.apcata.2023.119383>

This is a PDF file of an article that has undergone enhancements after acceptance, such as the addition of a cover page and metadata, and formatting for readability, but it is not yet the definitive version of record. This version will undergo additional copyediting, typesetting and review before it is published in its final form, but we are providing this version to give early visibility of the article. Please note that, during the production process, errors may be discovered which could affect the content, and all legal disclaimers that apply to the journal pertain.

© 2023 Published by Elsevier.

**Production of a high molecular weight jet-fuel precursor from biomass derived furfural and 2-methylfuran using propyl sulfonic SBA-15 catalysts**

**M.S. Zanuttini<sup>a</sup>; L.G. Tonutti<sup>a</sup>; C.A. Neyertz<sup>a</sup>; C. Ferretti<sup>b</sup>; B.S. Sanchez<sup>a</sup>; B.O. Dalla Costa<sup>a</sup>; C.A. Querini<sup>a</sup>**

<sup>a</sup> Instituto de Investigaciones en Catálisis y Petroquímica (INCAPE) – CONICET/UNL, RN168, Km 0, (3000) Santa Fe, Argentina.

<sup>b</sup> Instituto de Química Aplicada del Litoral, IQAL, UNL-CONICET, (3000) Santa Fe, Santiago del Estero 2829, Argentina

**Corresponding Author:**

Maria Soledad Zanuttini  
szanuttini@fiq.unl.edu.ar  
Postal Address: RN168, Km 0, (3000) Santa Fe, Argentina.  
Tel: +54-342-4511370 int. 6032/6033

**Abstract**

An effective catalyst for the production of branched chain fuel precursors with 15 carbon atoms (C15) from low carbon number, biomass-derived molecules is reported in this work. It shows that SBA-15 silica with the incorporation of sulfonic groups (S15) is highly active and selective for C-C coupling at low temperature, without solvent and under simple reaction conditions, giving a C15 condensation product with high selectivity, greater than 95%, via hydroxyalkylation/alkylation (HAA) of 2-methylfuran (2-MF) with furfural (FAL). As water was determined to have a great negative influence on the stability of these catalysts, synthesis modifications and various post-synthesis treatments were tested to improve yield of C15. As a result, it was possible to improve up to 12% the efficiency of the reaction by

incorporating hydrophobic groups in the synthesis of sulfonic SBA-15 by co-condensation. This catalyst can be recovered and recycled, preserving its stability over multiple reaction cycles.

**Keywords: C-C coupling, SBA-15, Furfural, 2-methylfuran, biomass**

Journal Pre-proof

## 1. Introduction

The number of countries announcing strategies to achieve net zero emissions continues to grow. By 2050, global transport sector is expected to emit 0.7 Gt of CO<sub>2</sub>, a 90 % drop relative to 2019-2020 levels. However, transport modes are not decarbonizing at the same rate due to the difference in technology maturity. According to the International Energy Agency, CO<sub>2</sub> emissions from cars, vans and trains will cease by 2050, but heavy trucks, maritime transport and aviation emissions will still exceed 0.5 Gt of CO<sub>2</sub> [1]. This reflects that many of the technologies needed to reduce CO<sub>2</sub> emissions in long-distance transport are currently under development. Thence, great efforts have been made to demonstrate the potential of biomass lignocellulosic material to produce platform compounds for further upgrading to liquid biofuels. Nevertheless, these molecules, mostly furanic compounds, contain 5-6 carbons. This number is far below the requirements of diesel fuels. For this reason, it is imperative to develop new routes for the production of molecules compatible with C12-C15 diesel from the condensation of biomass-derived smaller molecules [2]. A C-C condensation process followed by hydrodeoxygenation (HDO) is required to achieve these biofuels. Aldol condensation, pinacol coupling, ketonization, and hydroxyalkylation/alkylation (HAA) are the most relevant C-C coupling methods reported. Among them, the HAA reaction of furfural (FAL) and 2-methylfuran (2-MF) was reported for the first time by Huber et al. [3]. The latter can be obtained by hydrolysis-dehydration of hemicellulose from nonedible biomass sources. 2-Methylfuran can be produced by a selective hydrodeoxygenation of furfural. Both compounds are already produced on a large scale [4]. Our group made a contribution in the development of the hydrodeoxygenation of FAL to 2-MF process. [5].

The 2-MF molecule undergoes electrophilic substitution at the 5-position of the furan ring in presence of a suitable electrophile [4]. An interesting fact is that furfural, the precursor of 2-MF on an industrial scale, can itself act as an electrophile to achieve the C-C coupling reaction. Besides, 2-MF molecule has the advantage that one of its two reactive carbon atoms in alpha position is protected by a methyl group, reducing the possibility of undesired side reactions [6]. Li et al. studied the hydroxyalkylation/alkylation (HAA) reaction with furfural and two of its derivatives: furan (decarboxylation product) and 2-MF (selective hydrogenation product). The reaction with 2-MF was more effective due to the higher electrophilicity conferred by the electron donating effect of the methyl group. In turn, they studied the effect of different carbonyl compounds (furfural, ethyl levulinate and acetone) on the HAA of 2-MF. Furfural presented the highest reactivity due to its aldehyde functionality

[6]. The HAA reaction of FAL and 2-MF in presence of an acid catalyst occurs in two consecutive substitution steps to produce first a C10 dimer and finally a trimer, a 15 carbon oxygenated fuel precursor (C15) (Figure 1). A water molecule is released in the course of the reaction [4]. The C15 must then undergo a hydrodeoxygenation (HDO) to be converted in the suitable biofuel paraffin.

Fundamental criteria to select the catalyst for HAA reaction should be considered. The catalyst must have strong acid sites [7]. As has been reported, Brønsted acid sites are necessary to polarize the carbonyl group of furfural, charging it positively for nucleophilic attack on the 2-MF molecule, whose furanic ring is rich in electrons to form the new C-C bond [2, 7, 8]. For instance, an activated carbon material was inactive for HAA, due to the absence of strong Brønsted acid sites and the presence of weakly acidic groups, unable to catalyze this type of reaction [2]. Al-MCM-41 has also showed poor activity, attributable to its low proportion of strong acid sites [9]. Hence, several homogenous acids and heterogeneous Brønsted acid catalysts were tested in the HAA reaction [10-13]. However, Lou et al. obtained relatively good results using a Zr/SBA-15 catalyst with Lewis acid sites [2]. Nevertheless, the reaction temperature was relatively higher than the one used in Brønsted acid catalyzed reactions, owing to the fact that activation of the carbonyl group with Lewis catalytic sites is more difficult than with protons from Brønsted acids. The reaction rate was very low with this catalyst, being necessary 15 h and 140 °C in order to obtain 95 % conversion. Despite this, the use of Lewis acids may reduce some undesired side reactions caused by acidic protons such as ring opening [8].

In addition, it is important to choose mesoporous materials since the main product is a rather large molecule, and mass transfer limitations within pores must be avoided. Samikanuu et al. observed poor HAA activity with microporous HZSM-5 zeolites due to steric limitations which did not favor the formation of the desired product [9]. In contrast, meso/macroporous sulfonic acid resins showed improved activity and HAA yields as the reaction was free from steric or shape selectivity constrains [7].

Other factors to take into account to select the appropriate catalyst are: i) it should favor the interaction with hydrophobic reactants; ii) operational stability; iii) the possibility of being reused several times [9].

In this work, the synthesis of jet fuel range branched cycloalkanes oxygenated precursors by solvent-free HAA of furfural and its hydrodeoxygenated product, 2-MF, was explored. Taking into account the requirements established by previous studies, sulfonic silicas were chosen. A mesoporous material such as SBA-15 silica, functionalized with propyl sulfonic

groups as Brønsted acid sites was employed. This type of material has structural and acid properties that can be tuned by adjusting syntheses conditions. The reuse of the samples was also investigated. Due to the detrimental effect of water formed during the reaction, the catalyst with the highest concentration of propyl sulfonic groups was hydrophobically modified by different methods and tested in reaction. The samples were also characterized before and after the reaction. Theoretical studies were used to explain the characterization results.

The subsequent hydrodeoxygenation of the coupling product will be analyzed in a later article.

## **2. Experimental**

### **2.1. Catalyst preparation**

#### *2.1.1. Sulfonic SBA-15 catalysts*

SBA-15 type silica with propyl sulfonic acid groups was synthesized according to a modified method previously reported [15]. 1.9 N HCl was employed as medium, Pluronic® P 123 as surfactant, tetraethylorthosilicate (TEOS) as silicon source, (3-mercaptopropyl)trimethoxysilane (MPTMS) as functional precursor and H<sub>2</sub>O<sub>2</sub> as oxidant. The synthesis was carried out at 40 °C for 4 h, preceded by 1 h of hydrolysis of TEOS. After that, a hydrothermal treatment for 24 h at 130 °C and extraction of the surfactant with ethanol in Soxhlet were done. The amounts of TEOS and MPTMS were adapted so as to obtain loads of 5, 10 and 15 mol% of functional groups, keeping constant the amount of silicon added. The catalysts were labeled S5, S10 and S15 respectively. For comparative characterization purposes, the non-functionalized SBA-15 silica was synthesized, for which neither MPTMS nor hydrogen peroxide was added and pre-hydrolysis was not performed. This material was labeled S0.

#### *2.1.2. Hydrophobicity modified Sulfonic SBA-15 catalysts*

Three different ways of incorporating hydrophobic groups were tested. For this purpose, the load of 15 mol% of sulfonic groups was adopted. Two different procedures were followed to incorporate hydrophobic groups employing methoxy trimethylsilane (Me<sub>3</sub>Si) as precursor. First, adding Me<sub>3</sub>Si by co-condensation together with MPTMS at the ripening stage, and then proceeding as usual. This catalyst was named as S15S+H. A second catalyst was prepared by grafting from S15 synthesized material. It was suspended in toluene and Me<sub>3</sub>Si

was added. The suspension was then kept under reflux for 3 h and later filtered, washed and dried. This material was labeled S15G. A third alternative was the use of a single bifunctional precursor (acid + hydrophobic sites), namely (3-mercaptopropyl)-methyltrimethoxysilane (SHMeSi). This was incorporated instead of MPTMS in the synthesis following the same protocol as S15 [15, 16]. The catalyst was called S15B

## 2.2. Catalyst characterization

Textural properties of the catalysts were studied by Nitrogen adsorption-desorption isotherms recorded at  $-196\text{ }^{\circ}\text{C}$  in a relative pressure ( $P/P_0$ ) interval between  $1 \times 10^{-3}$  and 0.975 in a Micrometrics ASAP 2020 equipment as previously reported [15]. Total pore volume was determined according to *Gurvich rule* at  $P/P_0 = 0.975$ ; surface area was calculated with the BET model and pore-size distribution was calculated employing the Broekhoff and de Boer (BdB) method on the desorption branch of the isotherm.

S/Si ratios were obtained by X-ray fluorescence (XRF) employing a Shimadzu EDX-720 equipment in energy dispersion mode. The samples were analyzed in solid state and a calibration curve was established with solids of known composition.

The mesoscopic ordering was studied by small-angle X-ray scattering experiments performed at room temperature, in transmission configuration, with a fixed sample-detector distance of 1348.6 mm. The equipment employed was a XEUSS 1.0 (XENOCOS, France), with a Pilatus100K detector (DECTRIS, Switzerland) and a Cu  $K\alpha 1.2$  ( $\lambda = 1.5419\text{ \AA}$ ) X-ray source, in the Institute of Theoretical and Applied Physicochemical Research (INIFTA-CONICET-UNLP).

Due to the low thermal stability of the propyl sulfonic groups, the acid sites (SA) quantification by programmed temperature desorption of bases is not possible, therefore a volumetric method was employed [15]. Typically, 10-30 mg of solid were suspended in 20 mL acetonitrile and put under stirring while the potential was recorded with a LiCl saturated in ethanol electrode connected to a Metrohm 913 pH meter. Once the reading was stable, a solution of n-butylamine (0.01 M in acetonitrile) was pumped at a rate of  $0.1\text{ ml min}^{-1}$  while recording the potential. Once the potential had decreased and a clear plateau was reached, the analysis was finished. The equivalence point was determined by a Gran linearization method [17]. Briefly, the derivative of the potential as a function of the added volume added was obtained, and then a plot of its inverse divided by the total volume (initial plus added volume) vs added volume was built. A linear zone can be found, whose regression intersects the X-axis at the equivalence volume.

The nature of the acid sites was studied by infrared spectroscopy with pyridine as test molecule (Py-FTIR). Typically, a background spectrum of a self-supporting disk of pure sample (25-30 mg) was obtained at 25 °C after vacuum pretreatment at 300 °C for 1 h (10 ° min<sup>-1</sup>). Afterwards, the samples were heated to 150 °C and exposed to pyridine vapor during 1 h, followed by a vacuum purge for 1 h at the same temperature, to remove the physisorbed base. Again, a spectral collection was performed after the sample was cooled back to 25 °C. A similar procedure was carried out at 300 °C to obtain strong acid sites. Spectra were processed considering the subtraction of the sample background before pyridine adsorption.

Residual carbons on catalysts after reaction were characterized by FTIR using the standard KBr pellet technique. Also, the liquid samples of furfural, 2-MF, initial mixture and conversion products at 50% and 80% were studied with NaBr windows. All IR spectroscopy analyses were performed with a Shimadzu Prestige device with accumulation of 50 scans and 8 cm<sup>-1</sup> resolution.

Thermogravimetric analyses (TGA) were performed on a Mettler-Toledo TGA/SDTA851<sup>e</sup> module. Approximately 10 mg of sample were loaded into an alumina crucible and heated from 20 to 750 °C at 12 °C min<sup>-1</sup> with a N<sub>2</sub> flow rate of 50 mL min<sup>-1</sup>. Differential thermal gravimetric profiles (DTG) were obtained from the TGA profiles.

As an additional thermal characterization, temperature programmed stripping was performed to detect non-extracted surfactant and functional groups [18]. Typically, 10 mg of sample were loaded in a quartz cell and subjected to nitrogen flow (30 mL min<sup>-1</sup>). The cell was heated at 12 °C min<sup>-1</sup> from 25 to 850 °C while monitoring the output flow with a FID detector.

The hydrophobic-hydrophilic property of a solid surface determines the affinity of the solid with molecules of different polarity. Hydrophilic solids interact strongly with polar molecules such as water. Because of this, the adsorption isotherms of water have been used as a tool to have a measure of this property. In this work, hydrophobicity of the materials was assessed by water sorptometry at 24.7 °C in a relative pressure ( $P/P_0$ ) interval between 0.0 and 0.9 in a Dynamic Vapour Sorption Instrument model Advantage 1 (Surface Measurement Systems Ltd, London, UK). The device consists on a microbalance inside a thermostated chamber under nitrogen flow. Prior to the chamber, nitrogen flowed through a humidification stage to achieve the target partial pressure, and water adsorption on the sample was determined gravimetrically. Briefly, approximately 10 mg of the sample were loaded on the microbalance and then dry nitrogen flowed until the first equilibrium point was

reached, established when weight change was below  $10^{-3}$  wt.% min<sup>-1</sup>. Then, water partial pressure was increased stepwise, reaching successive equilibrium points under the same weight change criterion.

Fresh and used samples were observed both by Transmission Electron Microscopy (TEM) and by Field-Emission Scanning Electron Microscopy (FE-SEM). The equipment used is a high-resolution Transmission Electron Microscope Jeol JEM-2100 Plus. Also, a Zeiss Cross Beam 350 Scanning Electron Microscope was used. The acceleration voltage used was 2 kV. Portions of the samples were mounted on graphite tape. Additionally, the two microscopes are equipped with an Energy-Dispersive X-ray Spectroscopy (EDS) detector.

### **2.3. Reaction tests. Hydroxyalkylation/alkylation (HAA) reaction**

The solventless HAA reaction of 2-MF with FAL was carried out in a 20 ml thick glass closed reactor equipped with a magnetic stirrer and a reflux system. The temperature was controlled with a thermostated water bath. In a typical reaction, the catalyst (5-20 mg), 0.77 g of furfural (8 mmol) and 1.32 g of 2-MF (16 mmol) were added into the reactor and stirred at 400 rpm, with controlled temperature (40 - 80 °C) for 0.25 - 4 h. After the desired reaction time, the reaction mixture was cooled to 4 °C, diluted in acetonitrile and centrifuged to separate the catalyst, in order to stop the reaction. The sample was stored at -19 °C. The effects of reaction time, temperature, catalyst-reactant ratio (mg of catalyst per mol of 2-MF), or AS/FAL molar ratio (%mol of acid sites), 2-MF/FAL ratio, and water presence were studied. Each sample was diluted 500 times in acetonitrile and analyzed by gas chromatography in a Perkin Elmer Clarus 500 GC equipped with a MEGA-1 column (0.25 mm internal diameter, 0.15 µm film thickness and 60 m length) and a FID detector. The GC injector port and the detector temperature were set at 250 °C while the column temperature was set at 60 °C for 5 min, and then ramped from 60 to 250 °C at 10 ° min<sup>-1</sup>. Helium was used as carried gas. The main products were identified with GC-MS with an HP-5 column (0.35 mm internal diameter, 0.25 µm film thickness and 30 m length) set at 40 °C for 5 minutes and then ramped from 40 to 300 °C at 10° min<sup>-1</sup>. Since a sealed reactor was used and due to the high volatility of both reactants there was an increase in pressure as the reaction temperature was increased.

Conversion, product selectivity and yield are defined as follows:

$$\%X_{FAL} = \frac{\sum_{i=1}^n (A_i RF_i)}{\sum_{i=1}^n (A_i RF_i) + A_{FAL} RF_{FAL}} 100 \quad \text{Equation 1}$$

$$\%S_{C15} = \frac{A_{C15} RF_{C15}}{\sum_{i=1}^n (A_i RF_i)} 100 \quad \text{Equation 2}$$

$$\%Y_{C15} = \%X_{FAL} S_{C15} \quad \text{Equation 3}$$

where  $\%X_{FAL}$  = Furfural conversion,  $S_{C15}$  = Selectivity to C15,  $Y$  = C15 yield,  $i$  = product,  $A$  = chromatogram area,  $RF$  = response factor.

The molar response factors, relative to furfural, were measured using chromatographic standards of each compound. Solutions of furfural/octanol were prepared with different molar ratios. Each dilution was injected into the gas chromatograph (GC) four times, calculating the ratio of the area of the peaks and its average value. Subsequently, the area ratio was plotted against the molar ratios to obtain the slope, which represents the relative molar response factor (RF). This procedure was used to obtain the RF for furfural, 2-methylfuran and C15 compounds, resulting to be 3.51, 4.33 and 0.36 respectively. These values are referred to octanol. The normalization of these values taking as reference that of furfural, makes it possible to obtain the molar response factors relative to furfural, resulting to be 1.00, 1.23 and 0.10, respectively for furfural, 2-methylfurane and C15. There are few other peaks in the chromatogram, that are lumped as "other" compounds. These compounds have been analyzed by GC-MS resulting to be plurialkylated dimers. For this group of components, the response factor obtained for C15 was also used. As shown below, the amount of these compounds is relatively small, and therefore the uncertainty introduced by the use of this response factor does not have a significant impact on the calculation of conversion and selectivity. In all cases, it is assumed that the sum of FAL, C10, C15, 2-MF, and "Others" is 100 %.

The response factor takes into account the molecular weight of each compound, i.e., the terms  $(A_i RF_i)$  is proportional to the number of mol of compound  $i$ . To measure the reproducibility and calculate the confidence intervals of the results, the experiments were performed in triplicate and each reaction sample was analyzed 3 times by GC-FID. The 95 % confidence intervals were calculated with this information.

## 2.4. Theoretical studies

The geometry optimizations of reactants (2-methylfuran with furfural) and products (C10 dimer and C15 trimer) were carried out by DFT theory using the B3LYP correlation function

with a 6-31G(d,p) basis set. Frequency calculations allowed us to verify the minimum energy geometries and to analyze the IR vibrational frequencies of the groups of atoms present in each molecule. To compare with the experimental frequencies, theoretical values were scaled with a factor of 0.964 [19]. Besides, molar volume calculations were performed to characterize the molecular dimension of each species. All of these calculations were carried out using Gaussian 09 program package [20].

### 3. Results and Discussion

#### 3.1. Propyl sulfonic functionalized SBA-15: Characterization

Table 1 shows the characterization results obtained for the non-functionalized SBA-15, S0, and for the functionalized catalysts S5, S10 and S15.

The theoretical values of the S/Si ratios are higher than the experimental values determined by XRF. These results indicate that the incorporation of the functional groups was not complete, and the extraction could have eliminated some of them not linked to the solid structure. N<sub>2</sub> sorptometry analyses for S5, S10 and S15 resulted in type IV isotherms (Supplementary material Figure S1.A), typically associated with mesoporous materials, which exhibit the characteristic hysteresis loops of large mesopores. The BET surface area was high in all of these materials and the functionalization did not change the pore diameter, which exhibited a sharp distribution (Figure S1.B).

The small-angle X-ray diffraction scattering patterns of S0, S5, S10 and S15 are shown in Figure S2 of the Supplementary Material. The positions of the peaks of the indexed planes follow the typical pattern of a hexagonal-2D structure:  $q_{100}:q_{110}:q_{200}:q_{210}:q_{300} = 1:\sqrt{3}:2:\sqrt{7}:3$ , characteristic of SBA-15 materials. Derived structural parameters, such as d-spacing, lattice constant ( $a_0$ ) and pore wall thickness are presented in Table 1. The interplanar distance  $d_{100}$  was obtained as  $2\pi/q_{100}$  and, since the structure is hexagonal, the lattice constant  $a_0$  results  $d_{100} \cdot 2/\sqrt{3}$ . For S15, a decrease in the intensity and a widening of these peaks was observed, indicating a detriment in the ordering of the material. For this reason, the idea of using higher loads of propyl sulfonic groups in the synthesis was dismissed [15]. Furthermore, it was shown that slightly higher amounts of functional precursors have led to poorly ordered materials. Functionalized materials presented slightly higher lattice constant than S0, which together with a similar pore diameter, resulted in thicker walls.

The amount of acid sites determined by potentiometric titration with n-butylamine increases with the amount of MPTMS added in each case, and is consistent with the

experimental S/Si ratios. Figure 2 shows the study of surface acidity by Pyridine-FTIR for samples S5, S10 and S15 after evacuations at 150 °C. Adsorption bands on Brønsted acid sites assigned to N-H bending of pyridinium ion (PyH<sup>+</sup>) (1635 and 1547 cm<sup>-1</sup>), and the sum of Brønsted and Lewis acid sites (1489 cm<sup>-1</sup>) are observed after evacuation at 150 °C [21-23]. Bands at 1597 and 1446 cm<sup>-1</sup> could be assigned to H-bonded pyridine species [21]. Mauder et al. confirmed by <sup>15</sup>N COPMAS NMR the presence of pyridine adsorption on acid functionalized SBA-15 as hydrogen-bonded complexes with surface silanols in addition to ionic hydrogen-bonded complexes with functional groups (Brønsted sites) [24]. However, other authors assigned the aforementioned bands (1597 and 1446 cm<sup>-1</sup>) as pyridine coordinately bonded to Lewis acid sites [22, 23, 25]. To compare the acidity of the catalysts, the ratios of Brønsted band (1547 cm<sup>-1</sup>) were obtained, considering S15 absorbance ( $A_{S15}$ ) as reference. The results demonstrate that S10 and S5 have 0.71  $A_{S15}$  and 0.55  $A_{S15}$ , respectively. Similar values were obtained for the potentiometric titration ratios with S15 as reference (0.75 and 0.59 for S10 and S5 respectively). These results allow us to postulate that most of the surface acidity could be ascribed to Brønsted acid sites. Brønsted acidity was proportional to the S/Si ratio obtained by XRF. The Py-FTIR study after evacuation at 300 °C (not shown) displayed similar bands than after evacuation at 150 °C with very low intensity that could be assigned to a strong Py-sample interaction.

Figure 3 shows the first derivative of the weight loss curves (DTG) obtained by TGA for the fresh SBA-15 with different loads of propyl sulfonic groups: S5, S10 and S15, as they were used in the reaction. The DTG profiles are consistent with the N<sub>2</sub> stripping profiles already published in a previous work [18]. The peak around 77 °C corresponds to adsorbed water and residual ethanol that could have remained from the extraction process. As discussed in previous works [15, 18], propyl sulfonic groups decompose around 500 °C while non-oxidized propyl mercaptan groups decompose around 350 °C, and remaining surfactant burns mainly between 200 and 300 °C, with peaks at higher temperatures when the extraction is more extensive. The absence of peaks between 150 and 400 °C confirms the complete oxidation of the mercaptan precursors to sulfonic groups during the synthesis, as well as the complete extraction of the surfactant.

Additionally, TEM analysis provided both transverse and longitudinal views of the nanostructured SBA-15 silica channels. Both fresh (Figure 4A) and S15 (Figure 4B) samples were analyzed. No significant differences were observed between these two catalysts. On the other hand, SEM analysis revealed the organized structure of the silica in the form of longitudinally arranged nanorods, with an approximate length of 0.8-1 μm. (Figure 4C, S5

catalyst). In particular the S15 sample, characterized by a higher initial loading of mercaptan groups, exhibited a slight tendency towards agglomeration compared to the other samples, as shown in Figure 4D. In all the samples, the nanorods appeared to be interlocked with each other, forming a cohesive network. For S15, although the shape of the nanorods is similar to the other samples, the length of them is smaller (0.4-0.5  $\mu\text{m}$ ). Although there are no additional evidences, it is likely that the shorter nanorods observed in the S15 compared to the S5 might have been caused by the higher concentration of the sulfonic precursor. This difference in rod size may explain the better reaction results as a consequence of the reduced resistance to mass transfer in these shorter channels. Overall, the combined analysis of the SEM and TEM images provided valuable insights into the structural organization of the SBA-15 silica, highlighting the effects of different parameters such as initial group loading.

### 3.2. Propyl sulfonic functionalized SBA-15: Reaction Tests

In order to probe the catalytic potential of the propyl sulfonic functionalized SBA-15 catalyst for solvent-free C-C coupling of 2-MF and FA, different catalytic tests were performed.

#### 3.2.1. Effect of the load of propyl sulfonic groups

Figure 5 shows the results obtained with S0, S5, S10 and S15 at 60 °C at the same catalyst/FAL ratio ( $\text{mg cat. (g furfural)}^{-1}$ ) after 2 h of reaction. Through GC and GC-MS analysis, the main detected products were the desired trimer, C15, and a C10 dimer. Furthermore, the compounds referred to as 'others' are primarily plurialkylated dimers, likely resulting from the reaction of 2MF with furfural or with another 2-MF molecule. Sample S0 showed 1.3% conversion and a C15 yield of 0.26%. For all of the functionalized samples, the selectivities to C15 were very similar (95-97%) under the tested conditions. The lower yield observed with S5 compared to S10 and S15 can be explained in terms of the weak Brønsted acid sites/Furfural molar ratio, that is, the number of acid sites available to catalyze the reaction. In the case of S15, the molar ratio of acid sites/FAL was 0.39 mmol of acid sites per mole of furfural (0.039 mol%), while for S10 and S5, this ratio was 0.028 mol% and 0.021 mol%, respectively. Although it is a sequential reaction (Figure 1), the amount of dimer C10 detected in the presence of catalyst under these conditions was low, close to 2% as it is shown in Figure 5. This indicates that the second step, that is the reaction of the dimer

with 2-MF, is a very fast reaction.

Figure 5 shows the 95 % confidence intervals in the conversion, selectivities and yield. In the case of the conversion the confidence intervals are not higher than 7 %, and in the other cases they are smaller than 5 %, being smaller than the bullets used in Figure 5. Therefore, in the results shown in the figures discussed below only the confidence interval corresponding to the conversion are shown.

In addition, these catalysts were compared at a similar (acid sites/FAL) molar ratio (AS/FAL) (Figure S3 of the Supplementary Material). It can be observed that even in this condition, catalyst S15 showed the best performance. The confidence intervals are shown, and indicate that the results are statistically different. These results suggest that the acid site density is playing an important role in the activity of this catalyst. This is consistent with the fact that it is a bimolecular reaction and therefore, needs the interaction of both reactants in order to generate the products. Another important issue is that, as shown in the SEM images, there is a difference in the length of the S15 nanorods, and consequently, this change in the morphology can potentially improve the reaction performance leading to a decrease in the resistance to mass transfer.

### 3.2.2. Effect of reaction time

Figure 6 shows FAL conversion, selectivity and yield to the desirable C15 trimer for catalyst S15 under different conditions. The effect of reaction time was evaluated for S15 at 50 °C, a ratio of acid sites/furfural (AS/FAL) of 0.14 mol% and a stoichiometric ratio of the reactants. Reaction results obtained during 4 h are shown in Figure 6A. It was determined that the conversion increases with the reaction time up to 2 h, but the selectivity to C15 remains practically unchanged. A very high conversion was obtained for FAL, being approximately 98% at 2 h. After this reaction time, the conversion and selectivity showed no appreciable changes. These results show that C15 is stable and does not reconvert to lighter compounds and if there are parallel reactions to HAA, these are negligible even at long reaction times. The concentration of C10 dimer was 9.17% after 15 min of reaction and decreased until it stagnated at 2.4% after 2 h. As the reaction proceeds, the reactants are consumed and the viscosity increases constantly owing to product formation with the consequent limitation of mass transfer, which hinders the access of the reactants to the active sites [8]. No phase separation was observed during the reaction. The 2-MF/FAL ratio changes remarkably with the reaction time. In this test, 2-MF/FAL ratio was 2 at the beginning of the reaction, after 15 min increases to 3, and reaches values close to 9 after 4

h of reaction (Supplementary Figure S4). However, no marked increase in selectivity towards undesirable compounds by 2-MF self-coupling reactions was observed. This may be because, although it increased with respect to furfural during the reaction, its residual amounts are very low.

### 3.2.3. Effect of temperature

Figure 6B shows the reaction results for S15 with AS/FAL ratio of 0.037 mol % after 2 h, as a function of temperature. These low conversion conditions were chosen in order to observe differences. The conversion is favored by increasing the temperature from 40 to 60 °C, but above this temperature the conversion decreases. This is because at 60 °C, the reaction temperature is very close to the boiling point of 2-MF, so a greater fraction of it is in the vapor phase. The normal boiling point of 2-MF is 64 °C and 162 °C for the furfural. Therefore, at higher temperatures the effective concentration of 2-MF in the liquid phase becomes much lower than the nominal value and therefore there is a lower conversion. Balaskiran et al. established 65 °C as optimum temperature but they only tested the reaction at 45°C and 65°C [4].

### 3.2.4. Effect of acid sites to furfural ratio

Figure 6C shows the conversion, selectivity and yield to C15 after 2 h of reaction at 50 °C for different S15 catalyst loadings, and therefore different AS/FAL ratios. The furfural conversion increased up to ratios of 0.2 mol% of AS/FAL but the selectivity to C15 remained almost unchanged. Thus, the highest C15 yield was obtained with an AS/FAL ratio of 0.2%mol. Excess of catalyst under these conditions leads to higher conversions but also to higher selectivity towards lighter products which are undesirable. Hence, it appears to be an optimal ratio of acid sites/reactant that maximizes the yield of the desired product. Working with Zr/SBA-15 catalyst, Luo et al. [2] found similar results. Above a certain value, the increase in the amount of catalyst generates a decrease in conversion due to limitations of mass transfer between the catalyst and the reagents as a result of viscosity upsurge. In addition, in catalyst excess the probability of activating undesirable reactions, such as 2-MF molecules reacting with other 2-MF molecules, increases, as shown in section 3.2.5. As a consequence, there is a furfural remnant in the reaction system, lowering its conversion.

### 3.2.5. Methylfuran to furfural molar ratio effect

The effect of the initial molar ratio of the reactants was studied. Figure 6D shows catalytic test results obtained by adding the reactants at different proportions. The 2-MF/FAL ratio was varied from 0.5 to 4. It was observed that under certain conditions, the optimal yield of C15 was obtained when the reactant ratio was the stoichiometric one. Although the excess of 2-MF should have resulted in higher conversions, it generated a diluting effect on the catalyst that led to lower conversions. Furfural adsorption is disfavored when it is more diluted in 2-MF.

Furthermore, 2-MF/FAL ratios higher than 2 (stoichiometric value) slightly decrease the conversion and increase the yield of undesired dimers and heavier compounds, reducing the yield of C15.

Luo et al. observed a similar trend when using Zr/SBA-15 [2]. However, they found that when the amount of 2-MF increased, the viscosity of the mixture decreased slightly, improving the mass transfer efficiency between reactants and catalysts. Nevertheless, 2.5 was the optimal 2-MF/FAL ratio proposed. With higher values there were no significant improvements.

Therefore, in order to learn more about the reagent-catalyst interaction, some additional experiments were carried out. The results of these tests were analyzed with GC and GC-MS. One experiment was conducted as follows: Pure furfural and S15 catalyst were loaded into the reactor with a ratio of 5 mg Catalyst/g furfural. The reaction proceeded at 60 °C for 2 h. No conversion was observed. The other one was performed by reacting pure 2-MF in the presence of S15 under the same conditions. A conversion of 44 % to C13 poly alkylated dimers was observed (92% is 2,2' isopropylidenebis-5-methylfuran) and only 0.13 % was converted to trifurylmethane, C15. Evidently, the 2-MF molecule has a great capacity to undergo C-C coupling to give C13 alkylated dimers, but it requires a nucleophile such as furfural to guide selectivity towards the formation of larger molecules. Balakrishnan stated that, in the absence of furfural, 2-methylfuran itself acts as an electrophile in presence of water, by *in situ* generation of aldehyde functionality after ring-opening hydrolysis [4]. These authors observed a detriment in the yield of C15 at prolonged reaction times due to secondary reactions.

However, in the presence of the two reactants, Furfural and 2-MF, this C13 dimeric compound is not observed as a product. In addition, a reaction was performed using the C15 trimer contaminated with 3.2 % C10 dimer, 2-(2-furanylmethyl)-5-methyl-Furan, as reactant to determine possible decomposition or cracking reactions. Under these conditions, negligible changes were observed in the sample after 2 h at 60 °C.

Based on these studies, it is conceivable that, in the presence of the two reactants (2-MF and FAL), there are parallel reactions to HAA but that they are much slower.

In conclusion, the optimal conditions (conversion of 99.4 % and yield to C15 of 97.4 %) were obtained at 60 °C after 2 h of reaction with stoichiometric feeding of the pure reactants (without solvents) and a catalyst load of 2 % with respect to furfural, which represents 0.7 % of the total mass of reactants loaded into the reactor.

These conditions are simple and the catalyst loadings are compatible with the quantities used in the industry, indicating that this process is sustainable and suitable to be scaled up.

### 3.2.6. *Water effect*

To evaluate the effect of water in the reactor feed stream, a series of reaction tests were performed. Three catalytic tests were implemented by adding different amounts of water in the reaction together with the reactants at initial time of the reaction. The amounts of added water were calculated as percentage of the total liquid mass fed to the reactor. The selected reaction conditions were: stoichiometric ratio of the reactants, SA/FAL molar ratio of 0.039 mol%, 60 °C, 2 h, with the addition of 1, 4, and 10 % of water at the beginning of the reaction.

The desirable reaction is a consecutive reaction that generates one molecule of water for each molecule of C15 trimer. Without adding water to the system, that is, when pure furfural and 2-MF were fed to the reactor, furfural conversion and C15 selectivity were 61 and 96 %, respectively. After 2 h of reaction, 9.8 mmol of C15 and water are generated under these conditions. Taking these values into account, an experiment was carried out by adding this amount of water at the beginning of the reaction. This represents 4 % of water in the initial feed to the reactor. The results obtained in this case were 4.5 % conversion (a drop of 92 %) and 95 % selectivity to C15 after 2 h (See Figure 7).

By adding 1 % of water at the beginning of the reaction, there was a reduction of 38 % on the conversion after 2 h compared to the anhydrous situation and the selectivity was 94 %. When 10 % of water was added, the conversion dropped drastically to less than 1 %. Water, being one of the reaction's final products, modifies the reaction progress. However, another reason could be that water influences the interaction between catalytic sites and the reactants, affecting the efficiency of the catalyst. In order to verify this hypothesis, catalyst S15 was treated with water at 60 °C for 2 h and dried in an oven at 80 °C and then it was tested in reaction. The results were similar to those obtained without treatment with water. Similar findings were reported by Margolese et al [14]. That is, the stability of the catalysts after treatment with water has been tested and does not affect their subsequent

performance, but the presence of water in the reaction medium can affect the catalytic surface and its interaction with the reagents. Water interacts with silanol groups generating solvated sulfonic acid species as it was stated by Mauder et al. [24]. On the other hand, 2-MF itself can suffer opening hydrolysis in the presence of water [4].

The equilibrium limitation due to the presence of water is ruled out, since the equilibrium constant for the reaction under study is very high, as it is shown below using DFT calculations.

In conclusion, water in the feed highly affects the reaction results when using propyl sulfonic SBA-15. These results show that it is very important to dry the reactants in order to improve the conversion in this system, moreover taking into account that the FAL obtained from lignocellulose contains water. An alternative could be to operate under vacuum conditions to remove the water as it is generated, but this possibility is not feasible due to the high vapor pressure of both reactants.

### *3.2.7. Comparison of SBA-15 with another catalysts*

Table S1 (Supplementary material) shows results obtained in the present study with sulfonic functionalized SBA-15 catalysts with those previously reported by other authors. There is only one study in which a similar yield to that obtained in this work is reported (Yan et al., see Supplementary Material). However, in the study of Yan et al. the reaction was carried out using 10 mg of catalyst per mmol of furfural at 80 °C, while in this work, the catalyst loading was approximately 2 mg per mmol of furfural, and the reaction temperature was 60 °C. The information presented in Table S1 shows that the yield obtained with the functionalized SBA-15 catalyst is better than those already reported.

### **3.3. Hydrophobically modified propyl sulfonic SBA-15: Characterization and reaction tests**

The effect of the hydrophobicity of the catalyst was studied. For the S15S+H catalyst, the incorporation of hydrophobic groups was carried out by co-condensation adding  $\text{Me}_3\text{Si}$  together with SHSi in the maturation stage. Catalyst S15G was prepared incorporating the sulfonic groups by co-condensation followed by addition of the hydrophobic groups by grafting, and finally, S15B was synthesized using bifunctional SHMeSi groups.

Table 2 compares the acidity values and the activity results under the same reaction conditions for S15, S15B, S15G and S15S+H. The sample S15B incorporated less amount of S and therefore, it has lower acidity than the others. This may be due to the fact that the bifunctional precursor has only two ethoxide groups that bind to the silica, instead of the three groups of the usual precursor. On the other hand, the hydrophobicity generated by the group itself can cause additional interactions at the interface between the precursor solution and the surfactant micelle during synthesis, orienting the hydrophilic chains outwards, hindering their incorporation. The S15, S15S+H and S15G materials incorporated similar amounts of S. Figure 8 shows the TGA profiles of all the samples. These graphs were achieved after saturating the fresh samples with water. Since profiles exhibited major differences in humidity and carbon content, the weight losses were referred to the final mass, that is, to the weight of the silica support. Fresh catalysts were purposely moisturized by exposing them to saturated air at room temperature, and the water uptake was obtained from weight loss below 125 °C. The peak at 475 °C is assigned to the propyl sulfonic groups. The water sorption peak at temperatures below 125 °C in catalysts S15 and S15G are very similar. It can be appreciated that, although water sorption is high in catalysts S15, S15G and S15S+H, it was 20 % lower for S15S+H [16]. Besides, the peak at 475 °C in S15S+H is slightly higher, which is in agreement with the value of acid sites obtained by potentiometric titration (see Table 2). Larger differences were observed in the S15B catalyst prepared with the bifunctional precursor. The peak at 475 °C pose a smaller area, in agreement with the value of acid sites obtained with potentiometric titration. Furthermore, a peak appears in this catalyst at 270°C which is assigned to some remaining surfactant.

Sorption curves obtained by water sorptometry (Figure 9) show similar behaviors for S15, S15G and S15S+H, revealing that hydrophobicity of the porous surface was not enhanced by the addition of Me<sub>3</sub>Si. In contrast, S15B, where due to the use of a bifunctional precursor it is assured that each acidic group is neighboring to a methyl group, presented a rather hydrophobic character before the capillary condensation of water occurred. Previous studies in our group showed that S15S+H type of catalyst is preferentially distributed in non-polar phases, compared to S15 which has a higher affinity for polar phases [16]. Therefore, the incorporation of Me<sub>3</sub>Si seems to be preferential for the external surface of the particles, modifying the hydrophobic character on a macroscopic scale. Conversely, SHMeSi is more evenly distributed on the surface, conferring hydrophobicity to the pores walls. Since the synthesis of SBA-15 under the employed conditions follows a cooperative self-assembly

mechanism, where the P123 micelles point the hydrophilic portions outwards, it is reasonable to consider that the incorporation of Me<sub>3</sub>Si into the pore walls results hindered.

These samples were also studied by Py-FTIR as shown in Figure 10, showing the same bands as mentioned above. Considering the absorbance of S15 ( $A_{S15}$ ) at 150 °C as representative of the concentration of acid sites, the acidity of S15B+H, S15G and S15B are 0.60  $A_{S15}$ , 0.58  $A_{S15}$  and 0.33  $A_{S15}$ , respectively. On the other side, the ratios obtained by potentiometric titration were 0.94  $A_{S15}$ , 0.89  $A_{S15}$  and 0.39  $A_{S15}$ . Even though the values are different for these acidity analyses (Table 2), they have the same trend, with similar value for S15H+B and S15G and lower for S15B. There seems to be no correlation between acid strength and the reaction results. However, the idea that the acid sites in the S15B+H catalyst are preferentially located on the outer surface explains this apparent contradiction. These sites are easily accessible and correspondingly more active.

TEM and SEM images indicate that no significant differences were observed in terms of morphology of the nanorods or the channels of the samples.

The two last rows of Table 2 show the conversion and C15 yield values obtained with all these catalyst after 2 h at 60 °C. Reaction conditions were chosen so that the conversions were less than 100 %, in order to better observe the differences. Catalyst S15B achieved lower conversions and yields than S15 under the same reaction conditions. This is attributable to the fact that S15B incorporated a lower amount of sulfur and consequently presented fewer acid sites per gram of catalyst. In the case of catalyst S15G, although it presented less water adsorption than S15, the incorporation of acid groups did not completely reach the desired values, and therefore the conversions achieved were lower. Catalyst S15B+H achieved a 5% higher conversion than S15. These results indicate that the better performance could be attributed to the presence of hydrophobic groups, since the amounts of S incorporated were similar to those of S15 catalyst. The turnover number (TON) is the highest for the reaction catalyzed by S15B+H.

Furthermore, catalysts S15 and S15B+H were tested under higher conversion conditions (60 °C, 2 h, 2-MF/FAL = 2, 0.43 mg cat/mmol FAL) and similar trends were obtained. The conversions obtained were 69 % with S15, and 79 % with S15B+H, which represents a 14.5 % improvement under these conditions. Regarding selectivity, no significant differences were observed between both materials.

In a previous section, the detrimental effect of water on the catalysts has already been discussed. When comparing the effects of 1 % and 4 % of water in the feed, it was observed

that the activity of S15 decreased 38 and 92 %, respectively (Figure 7), and for S15S+H, the conversion diminished 31 and 74 %, respectively (Supplementary Figure S5). Hence, the modification of hydrophobicity in the synthesis improves the catalytic performance. One of the reasons may be precisely that the incorporation of hydrophobic groups improves the stability of the catalyst by preventing water from interfering with the propyl sulfonic groups. Consequently, the hydrophobic reactants have better access to the active sites of the catalyst with functionalities of a similar nature [4]. Balakrishnan et al. analyzed the role of the alkyl linkers added to an amorphous silica on hydrophobicity and activity [4]. Two silica-supported sulfonic acid catalysts with alkyl-linkers and a sulfonic acid silica lacking an alkyl-linker were compared. Catalysts with alkyl linkers were more active than the catalyst without a linker because the alkyl linker provides better solubility of the sulfonic acid group in hydrophobic reactants. These authors also observed that C15 underwent side reactions under acidic conditions as it was also established in this article in previous sections. However, for a more hydrophobic environment of catalyst, product yields remained the same throughout the reaction. According to Mauder et al., water molecules are structured around sulfonic acid groups. This solvation could affect the reactivity and/or the access of the reactants to acid sites [24].

Figure 11 shows TGA and DTG profiles for fresh and used S15 and S15S+H. Regarding the weight losses above 125 °C, fresh S15 and S15S+H present the aforementioned peak centered around 475 °C related to sulfonic groups and representing weights of 13 % and 16 %, respectively. In contrast, used catalysts present noticeable higher losses, of 187 % and 197 %, respectively, which compress the overlapping of several signals, with the largest contributions centered around 300-350 °C and around 450-500 °C, and the peaks appeared at higher temperatures for the hydrophobic catalyst. Based on TGA, temperature programmed stripping and FTIR studies, it is evident that the reduction in catalyst activity was mainly due to the adsorption of organic molecules on the catalyst surface. Samikannu et al. obtained the same conclusion when using acid NbOPO<sub>4</sub> catalyst [9].

### 3.4. Theoretical characterization of reactants and products

In order to evaluate the molecular properties of the species involved in the synthesis reaction of fuel precursor, DFT studies were carried out. The optimized structures corresponding to 2-MF and FAL reactants, and C10 monomer and C15 dimer products are shown in Figure 12. From the geometric optimization of all these structures, the following intramolecular interatomic distances ( $d$ ) were obtained:  $d_{(C-C)} \approx 1.45 \text{ \AA}$ ,  $d_{(C=C)} \approx 1.36 \text{ \AA}$ ,  $d_{(C-O)}$

$\approx 1.38 \text{ \AA}$ ,  $d_{(C=O)} \approx 1.21 \text{ \AA}$ ,  $d_{(C-H)} \approx 1.09 \text{ \AA}$ , and  $d_{(O-H)} \approx 0.96 \text{ \AA}$ . These distances are in full agreement with the values reported in the literature [26-29].

The C10 monomer presented an O-C-C angle at the central carbon atom with the C atoms of the furan rings of  $\approx 112^\circ$ , and two intramolecular hydrogen bonds (H---O-H) of  $2.68 \text{ \AA}$  that play an important role in molecular stability. The C15 dimer, which contains a three-bladed propeller shape, has three C-C-C angles of  $\approx 112^\circ$  between the center carbon atom and the carbon atoms of furan rings.

Considering the molar volume ( $mV$ ;  $\text{cm}^3 \text{ mol}^{-1}$ ) of each molecule, it was possible to calculate the molecular volume ( $MV$ ;  $\text{\AA}^3$ ), with the Equation 4:

$$MV = (mV \times 10^{24} \text{ \AA}^3) / N_A \quad \text{Equation 4}$$

where  $N_A$  is Avogadro constant ( $6.023 \times 10^{23} \text{ mol}^{-1}$ ). Considering each molecule as spheres, the kinetic diameter ( $D$ ,  $\text{\AA}$ ) of each molecule was calculated with the expression (5):

$$D = 2 \sqrt[3]{(3 \times MV / 4\pi)} \quad \text{Equation 5}$$

and the results are shown in Table 3. All the kinetic diameter values are smaller than the pore diameter of the SBA-15 catalysts functionalized with propyl sulfonic acid (10 nm), so it is possible to understand that both the reactants and the products would not have dimensional limitations to enter and exit within the pores.

When the geometry of a molecule is optimized by DFT, the optimization energy ( $E$ ) is the minimum value of potential energy that this species presents and that corresponds to a stationary geometry. Similarly, the Gibbs free energy of formation of a compound ( $\Delta G$ ) is a thermodynamic equilibrium potential that, like  $E$ , is a measure of the chemical stability of a compound. For molecules with similar structures, it is possible to use the  $E$  and  $\Delta G$  values of each species to analyze their stability under standard conditions of pressure and temperature (SCTP) or under reaction temperature ( $50 \text{ }^\circ\text{C}$ ). Thereby, the sample with the lowest values of  $E$  and  $\Delta G$  between all possible ones would be the most thermodynamically stable [30, 31]. Table 3 shows the absolute values of  $E$  and  $\Delta G$  ( $\text{Kcal mol}^{-1}$ ) for reactants and products molecules. About the results, it can be noticed that the values of  $E$  and  $\Delta G$  increase as furan rings condense with methyl furan, generating a more stable species.

Based on these results, and trying to determine if the condensation reactions involving the consecutive substitution reaction between furfural and 2-methyl furan are favored, the variations of Gibbs free energy of reaction ( $\Delta G_R$ ) and the enthalpies of reaction ( $\Delta H_R$ ) for

each step were calculated. The results obtained are presented in Table 4. The  $\Delta G_R$  values for the condensation reactions studied resulted to be large negative numbers, confirming that the reactions are favored with a high equilibrium constant, while  $\Delta H_R$  values validate the experimental exothermic feature of these reactions [30, 31].

### 3.5. Reuse: Stability test

During the activity studies of the catalytic reaction, a decrease in activity was observed.

A simple observation of catalysts after reaction denotes carbon deposition, since the color turned black. In consequence, a regeneration treatment was necessary before reusing the catalysts. Since it is not possible to burn the deposits due to the inherent instability of the functional groups, solvent washing is required to remove the reactants and/or products adsorbed on the catalyst. The influence of the washing solvent in the regeneration treatment was studied. Hence, three equal catalytic tests were performed with S15. After each reaction the catalyst particles were separated by centrifugation, washed several times with a solvent, dried at 100 °C and analyzed by TGA. The conversions obtained were similar, around  $88 \pm 5$  %. Figure 13A shows DTG profiles of fresh S15 and three reused samples under the same reaction conditions: one subsequently washed with acetone, the other with acetonitrile and a third with ethanol 99%. The fresh catalyst shows a peak at low temperatures characteristic of water desorption and a peak around 480 °C, characteristic of the decomposition of propyl sulfonic groups. Used catalyst profiles show a low-temperature peak related to the remaining solvent and a shoulder around 330 °C and another between 460-500 °C, related to the decomposition of adsorbed reactant, products and/or acid sites. The comparison of the normalized profiles of the catalyst washed with the different solvents showed that the one washed with acetone desorbed a greater amount of compounds. The catalysts samples washed with ethanol and acetonitrile presented similar profiles. The N<sub>2</sub> stripping profiles were in agreement with these results (Figure S6 Supplementary material). The fresh catalyst shows a peak at 524 °C with a shoulder at 586 °C. The profile of the catalysts used and washed with the different solvents show that there are compounds that begin to desorb at 200 °C, with a peak at 440 °C and a shoulder at 524 °C, indicating that there are molecules that decompose before and together with the acid sites. As a result, acetonitrile was chosen as washing solvent.

To evaluate the operational stability of the catalysts, stability tests were conducted with S15 and S15B+H. After each reaction test, the solid catalysts were separated by centrifugation, washed several times with acetonitrile, dried at 100 °C and directly reused in

reaction. The results of the stability test for each catalyst are shown in Table 5. With the first use of S15, C15 yield was 70 %. After 3 reuse cycles of S15, product yield decreased by only 10 %. From the fourth cycle the conversion decreases significantly, being reduced by 80 % and after 5 cycles the catalyst is almost completely deactivated. In the case of S15S+H under the same conditions, the yield value of C15 in the first cycle was 77 %. In the first reuse, a higher yield of C15 was obtained, 83 %. After 3 cycles of S15S+H reuse, the yield remained the same and after the fourth cycle it decreased only 30 %. Balakrishnan also performed a stability test of an alkyl sulfonic amorphous silica [4]. The material was recycled 4 times without activity reduction but the conditions tested were with much higher excess of catalyst.

In the case of S15, the specific area after 5 reuse cycles was less than  $1 \text{ m}^2 \text{ g}^{-1}$ . This indicates that there is a large amount of adsorbed organic molecules that deactivate the catalyst, to the point of blocking silica channels.

While for S15S+H the specific area after 5 reuse cycles was  $137 \text{ m}^2 \text{ g}^{-1}$ , that is, it was reduced by 80 %, but it is still high enough to retain certain level of activity. The pore volume drops to  $0.1 \text{ cm}^3 \text{ g}^{-1}$ , it was reduced by 90 % and the average pore diameter was 5.4 nm, it dropped to half of the initial value.

To further understand the deactivation effects, the quantity of acid sites was measured after one and four cycles of reaction and catalyst washing. The values of the fresh and after one and four cycles were 1.18, 0.81 and  $0.5 \text{ mmol.g}^{-1}$  catalyst, representing a reduction of active acid sites of 32 and 57 %, respectively. Based on these data, it is not possible to determine if deactivation of the sites occurs due to leaching or coke deposition. However, the fresh catalyst is white, while it turns brown after being used and washed. Moreover, S (sulfur) was measured in a sample of undiluted reaction medium after 2 hours of reaction at  $60^\circ\text{C}$  using X-ray fluorescence. No S signal was observed, indicating that the amount is so small that it is below the detection limit of the equipment ( $<7 \text{ ppm}$ ). Thus, if there is any leaching, it represents a loss of less than 6% of the propylsulfonic groups due to this effect. Consequently, it can be inferred from these results that deactivation mainly occurs due to the blocking of sites on the catalyst. Furthermore, when comparing the fresh and used S15 samples, the SEM images revealed noticeable differences in the surface characteristics. While in the fresh SBA-15 sample (Figure 4E), the channels are visible on the external surface, rods surface of the used sample (Figure 4F) appeared to be rougher and with more defects, potentially indicating deterioration due to abrasion or the deposition of coke or reaction by-products. Unfortunately, TPO studies cannot be carried out due to the

overlapping profiles of the decomposition of the propylsulfonic acid groups and the oxidation of coke to CO or CO<sub>2</sub>, at similar temperatures.

Figure 13B shows the DTG profiles obtained by TGA for fresh S15 and used catalyst after the first cycle and after 4 cycles. These results show a clear increment of remaining compounds on the catalyst after 4 reuse cycles. This reinforces the idea that this is the cause of deactivation. Acid sites of the fresh catalyst S15 and after the first and the fourth cycle were measured by potentiometric titration. The values were 1.18, 0.8 and 0.5 mmol per g of catalyst, respectively.

In conclusion, catalyst-recycling studies revealed that both S15 and the hydrophobicity modified S15S+H catalyst, could be recycled 3 times with minor reduction of activity.

### **3.6. FTIR evaluation of liquid and solid phases during the reaction**

#### *3.6.1 FTIR evaluation of liquid reactants and products during reaction*

In order to evaluate the reaction of 2-MF with FAL to produce C15 product, liquid samples were characterized by FTIR. Considering that the functional groups involved in the identification of these compounds are present between 1900 and 500 cm<sup>-1</sup>, the FTIR spectra were recorded in this region and are shown in Figure 14A.

For the spectrum of Furfural (FAL spectrum in Figure 14A), the main characteristic bands are identified from 1700 - 1000 cm<sup>-1</sup>. The band at 1680 cm<sup>-1</sup> corresponds to C=O stretching vibration, while peaks at 1570 and 1470 cm<sup>-1</sup> correspond to the C=C stretching vibration of the furan ring, and 1390 and 1365 cm<sup>-1</sup> are attributed to C-H bending vibrations. The bands at 1277, 1157, 1078, 927, 883, 777 and 593 cm<sup>-1</sup> correspond to C-O, C-C=C, C-C-O, C-O-C stretching and bending vibrations present in the furan ring. In the spectrum of 2-Methyl Furan (2-MF spectrum in Figure 14A), the bands at 1603 and 1145 cm<sup>-1</sup> are assigned to stretching and bending vibrations of deformation C=C groups, respectively, present in furan ring and the bands at 1509 and 914 cm<sup>-1</sup> are assigned to bending of CH<sub>3</sub> associated with C=C bending and stretching vibrations of furan. The bands at 1454, 1386, 1373, 1235, 1213, 1082, 1016 and 887 cm<sup>-1</sup> correspond to C-O, C-C=C, C-C-O, C-O-C stretching and bending vibrations present in the furan ring; and the 795 and 728 cm<sup>-1</sup> are attributed to bending vibrations of CH<sub>3</sub> group.

In the spectrum of C15 trimer (which was synthesized and purified as indicated in supplementary information) it is possible to identify new bands at 1563, 1352, 1240, 1194, 1153, 1001, 963, 945, 924, 778, 735, 540 and 530 cm<sup>-1</sup>, associated to a greater extent with

the deformation of the coupled furan rings present in C15 trimer molecule. The bands at 1352, 964, 945 and 924  $\text{cm}^{-1}$  present in the spectrum are attributed to the stretching and bending vibrations of H-C-OH in C10 dimer molecule, which appear as a contaminant in the sample of C15.

The assignment of all bands present in the experimental spectra of FAL, 2-MF, C10 and C15 (Figure 14A) was validated by analyzing vibrational frequencies in the region 1900-500  $\text{cm}^{-1}$  of a theoretical spectra calculated at 25 °C by DFT (Figure 14B) and with data from bibliography [32-34].

The FTIR spectrum of the reactant mixture at the initial time of reaction clearly shows only the characteristic bands identified in the FAL and 2-MF spectrum ( $t_0$  in Figure 14A). As a result of the reaction between FAL and 2-MF, in the spectrum of samples at 50 % FAL conversion (spectrum  $X_{50\%}$  in Figure 14A), the bands at 1563, 1352, 1240, 1194, 1153, 964, 945 and 924  $\text{cm}^{-1}$  are evident, indicating the presence of the C10 dimer in the sample. The C10 presence in the FTIR spectra is consistent with the results of the reaction, where a small signal corresponding to this compound was observed by gas chromatography. In addition, bands assigned to the C15 trimer are observed, which also demonstrates its presence. As a result of the progress of the reaction, in the spectrum of the sample corresponding to a conversion level of 80 % (spectrum  $X_{80\%}$  in Figure 15A), an increase in the intensity of the bands present at 1563, 1240, 1153, 945, 778 and 540  $\text{cm}^{-1}$  assigned to C15 is observed, together with the decrease in the intensity of the bands present at 1352 and 964  $\text{cm}^{-1}$  attributed to C10. The presence of the band assigned to the C=O group in the samples corresponding to the conversion of 50-80 % indicates that furfural had not been completely converted yet.

### 3.6.2 FTIR evaluation of solid catalysts during reaction

On the other hand, catalyst samples were analyzed by FTIR after one and five reaction cycles of use and compared with fresh samples. The spectra are presented in Figure 15.

The broad band at 3425  $\text{cm}^{-1}$  corresponding to stretching vibration of silanol groups Si-OH, at 1099  $\text{cm}^{-1}$  of Si-O-Si stretching, at 800 and 471  $\text{cm}^{-1}$  of bending and out plane deformation of Si-O, and 960 of Si-OH stretching are observed for catalysts [35]. The bands at 2924 and 2855  $\text{cm}^{-1}$  of  $\text{CH}_2$  and 1636  $\text{cm}^{-1}$  of C-O are assigned to organic functionalized groups in fresh samples. After the reaction, a relative decrease of silanols band (3425  $\text{cm}^{-1}$ ) with respect to  $\text{CH}_2$  and the appearance of a peak at 1709  $\text{cm}^{-1}$  due to carbon deposition are observed. Similar results in decrease of silanols band intensity were observed for others

reaction with furfural and it could be related to the surface binding of the secondary molecules formed [34]. In these experiments, the water formed by condensation during reaction under solid acid catalysis conditions can produce secondary hydrolysis reactions that finally ended in humins covering the catalyst surface [34]. In consequence, the deactivation of the catalyst S15 with reuse cycles is evidenced by this FTIR study.

#### 4. Conclusions

The sulfonic SBA-15 catalyst resulted to be very active in the C-C coupling reaction and showed very good results compared to those published by other authors. Even more so, the fact that the reaction is carried out at low temperature and in the absence of added solvents is noteworthy. Using biomass-derived molecules of low molecular weight, it was possible to obtain compounds containing 15 carbon atoms, with selectivity higher than 95 %. This was achieved by the hydroxyalkylation/alkylation reaction of 2-methylfuran and furfural.

Water has a strong negative influence in the kinetics of this reaction, affecting the interaction between the acid sites and the reactants. In order to moderate this effect, catalysts with modified hydrophobicity were prepared using different procedures, such as modifications during or after the synthesis. The co-condensation of 3-mercaptopropyl-trimethoxysilane with methoxy-trimethylsilane was the more effective method to increase the hydrophobicity of the functionalized SBA-15 catalyst. With this change in the catalyst design it was possible to obtain 8 to 12 % better yields than in the case of catalyst without modification of its hydrophobicity.

The catalyst can be reused at least 3 cycles with low yield decrease.

The C-C coupling reaction used to obtain fuel precursors in this study has important advantages, being one of the more important that it is carried out under mild conditions, and that the reactants are fully renewable, obtained from biomass. Another aspect that can be highlighted is that the formation of secondary products is negligible in the selected and optimized reaction conditions. Even though the conversion and selectivity to the product containing 15 carbon atoms are very high, it is also relevant that the separation between this products and the small unconverted fraction of reactants is very easy, not only because of the difference between the boiling points, but also due to its polarity, being the reactants miscible with water, while the product is not.

## Acknowledgements

The authors wish to acknowledge the financial support received from Agencia Nacional de Promoción Científica y Técnica (PICT 2018-3634), Agencia santafesina de ciencia, tecnología e innovación (IO-2019-0092): and Universidad Nacional del Litoral (CAID 2021 50620190100154LI).

## CRediT author statement

M. S. Zanuttini: Methodology, validation, investigation, formal investigation; writing original draft, funding acquisition; C. Neyertz: Methodology, validation, investigation, formal investigation; writing-review& L.G. Tonutti: investigation, formal analysis, writing original draft; B.O. Dalla Costa: conceptualization, writing-review& editing; B. Sanchez: conceptualization, methodology, writing-review& editing; C. Ferretti: Formal analysis; Investigation; Methodology, Software, writing-review& Validation. A. Querini: supervision, funding acquisition, writing-review& editing,.

## REFERENCES

- [1] S. Bouckaert, A.F. Pales, C. McGlade, U. Remme, B. Wanner, L. Varro, D. D'Ambrosio, T. Spencer, Net zero by 2050: A roadmap for the global energy sector, A report of the International Energy Agency (2021). <https://www.iea.org/reports/net-zero-by-2050>.
- [2] Y.J. Luo, Y.H. Zhou, Y.B. Huang, Catal. Lett. 149 (2019) 292-302. <https://doi.org/10.1007/s10562-018-2599-6>.
- [3] A.V. Subrahmanyam, S. Thayumanavan, G.W. Huber, ChemSusChem 3 (2010) 1158-1161. <https://doi.org/10.1002/cssc.201000136>
- [4] M. Balaskrishan, E.R. Sacia, A.T. Bell, ChemSusChem 7 (2014) 1078-1085. <https://doi.org/10.1002/cssc.201300931>
- [5] M.S. Zanuttini, M. Gross, G. Marchetti, C. Querini, App. Catal. A 587 (2019) 117217. <https://doi.org/10.1016/j.apcata.2019.117217>
- [6] G. Li, N. Li, Z. Wang, C. Li, A. Wang, X. Wang, Y. Cong, T. Zhang, ChemSusChem 5 (2012) 1958-1966. <https://doi.org/10.1002/cssc.201200228>

- [7] L.J. Konwar, A. Samikannu, P. Mäki-Arvela, J.P. Mikkola, *Catal. Sci. Technol.* 8 (2018) 2449-2459. <https://doi.org/10.1039/C7CY02601C>
- [8] S. Li, N. Li, G. Li, L. Li, A. Wang, Y. Cong, X. Wang, G. Xu, T. Zhang, *App. Catal. B* 170-171 (2015) 124-134. <https://doi.org/10.1016/j.apcatb.2015.01.022>
- [9] A. Samikannu, L. J. Konwar, K. Rajendran, C.C Lee, A. Shchukarev, P. Virtanen, J.P. Mikkola, *App. Catal. B* 272 (2020) 118987. <https://doi.org/10.1016/j.apcatb.2020.118987>
- [10] H. Li, S. Saravanamurugan, S. Yang, A. Riisager, *ACS Sustainable Chem. Eng.* 3 (2015) 3274-3280. <https://doi.org/10.1021/acssuschemeng.5b00850>
- [11] G. Li, N. Li, J. Yang, L. Li, A. Wang, X. Wang, Y. Cong, T. Zhang, *Green Chem.* 16 (2014) 594-599. <https://doi.org/10.1039/C3GC41356J>
- [12] M.J. Climent, A. Corma, S. Iborra, *Green Chem.* 16 (2014) 516–547. <https://doi.org/10.1039/C3GC41492B>
- [13] Q. Deng, P. Han, J. Xu, J.J. Zou, L. Wang, X. Zhang, *Chem. Eng. Sci.* 138 (2015) 239-243. <https://doi.org/10.1016/j.ces.2015.08.025>
- [14] D. Margolese, J.A. Melero, S.C. Christiansen, B.F. Chmelka, G.D. Stucky, *Chem. Mater.* 12 (2000) 2448-2459. <https://doi.org/10.1021/cm0010304>
- [15] L.G. Tonutti, M.A. Maquiritain, C.A. Querini, B.O. Dalla Costa, *J. Porous Mater.* 30 (2023) 33-42. <https://doi.org/10.1007/s10934-022-01321-2>
- [16] M.A. Maquiritain, L.G. Tonutti, C.A. Querini, B.O. Dalla Costa, M.L. Pisarello, *App. Catal. A* 650 (2022) 119014. <https://doi.org/10.1016/j.apcata.2022.119014>
- [17] T. Michałowski, M. Toporek, M. Rymanowski, *Talanta* 65 (2005) 1241-1253. <https://doi.org/10.1016/j.talanta.2004.08.053>
- [18] L.G. Tonutti, B.O. Dalla Costa, H.P. Decolatti, G. Mendow, C.A Querini, *Chem. Eng. J.* 424 (2021) 130408. <https://doi.org/10.1016/j.cej.2021.130408>
- [19] A.P. Scott, L. Radom, *J. Phys. Chem.* 100 (1996) 16502-16513. <https://doi.org/10.1021/jp960976r>
- [20] M.J. Frisch, G.W. Trucks, H.B. Schlegel, G.E. Scuseria, M.A. Robb, J.R. Cheeseman, G. Scalmani, V. Barone, B. Mennucci, G.A. Petersson. *Gaussian 09*, Gaussian Inc., Wallingford CT, 2009. <http://gaussian.com/glossary/g09/>

- [21] B. Chakraborty, B. Viswanathan, *Catal. Today* 49 (1999) 253-260. [https://doi.org/10.1016/S0920-5861\(98\)00431-3](https://doi.org/10.1016/S0920-5861(98)00431-3)
- [22] N.V. Vlasenko, Y.N. Kochkin, G.M. Telbiz, O.V. Shvets, P.E. Strizhak, *RSC Adv.* 9 (2019) 35957-35968. <https://doi.org/10.1039/C9RA07721A>
- [23] J. Zhang, S. Yang, W. Cai, F. Yin, J. Jia, D. Zhou, B. Zhu, *Catalysts* 9 (2019) 770. <https://doi.org/10.3390/catal9090770>
- [24] D. Mauder, D. Akcakayiran, S.B. Lesnichin, G.H. Findenegg, I.G. Shenderovich, *J. Phys. Chem. C* 113 (2009) 19185-19192. <https://doi.org/10.1021/jp907058y>
- [25] X. Tian, H. Tian, *React. Chem. Eng.* 6 (2021) 1002-1015. <https://doi.org/10.1039/D1RE00020A>
- [26] Y. Yang, X. Wu, C. Liu, S. Huang, *Chem. Phys.* 443 (2014) 45-52. <https://doi.org/10.1016/j.chemphys.2014.08.008>
- [27] V.V. Atuchin, B.I. Kidyarov, B-O chemical bond length as a criterion for searching new acentric borate crystals. In *International. Workshop on Nonlinear Photonics* (pp. 1-3) 2011. <https://doi.org/10.1109/NLP.2011.6102667>
- [28] J.D. Larkin, K.L. Bhat, G.D. Markham, T.D. James, B.R. Brooks, C.W. Bock, *J. Phys. Chem. A* 112 (2008) 8446-8454. <https://doi.org/10.1021/jp800125p>
- [29] R. Chang, K.A. Goldsby, *Química*, 11th ed., McGraw-Hill Education, 2013.
- [30] J.B. Foresman, A.E. Frisch, *Exploring Chemistry with Electronic Structure Methods*, 3rd ed., Gaussian Inc., Wallingford, CT, 2015.
- [31] J.M. Smith, H.C. Van Ness, M.M. Abbott, M.T. Swihart, *Introduction to Chemical Engineering Thermodynamics*, McGraw-Hill Education, New York, 2018.
- [32] R.M. Silverstein, G.C. Bassler, T.C. Morrill *TC*, *Spectrometric Identification of Organic Compounds*, 5th ed., Jhon Wiley & Sons, New York, 1991.
- [33] H.K. Ong, M. Sashikala, *J. Trop. Agric. Food Sci.* 35 (2007) 305-312. <http://jtafs.mardi.gov.my/index.php/publication/issues/archive/40-2007/volume-35-no2/165-350213>
- [34] W. Wang, X. Ji, H. Ge, Z. Li, G. Tian, X. Shao, Q. Zhang, *RSC Adv.* 7 (2017) 16901-16907. <https://doi.org/10.1039/C7RA02396K>

[35] B. Shokri, M.A. Firouzjah, S.I. Hosseini, FTIR analysis of silicon dioxide thin film deposited by metal organic-based PECVD, in Proceedings of 19th International Symposium on Plasma Chemistry Society, Germany, pp.26-31 (2009).

### Legend to Figures

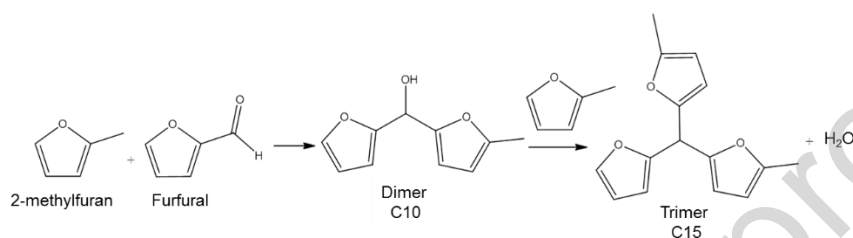


**Figure 1.** 15 carbon oxygenated fuel precursor (C15) synthesis by consecutive substitution reaction between furfural and 2-methylfuran.

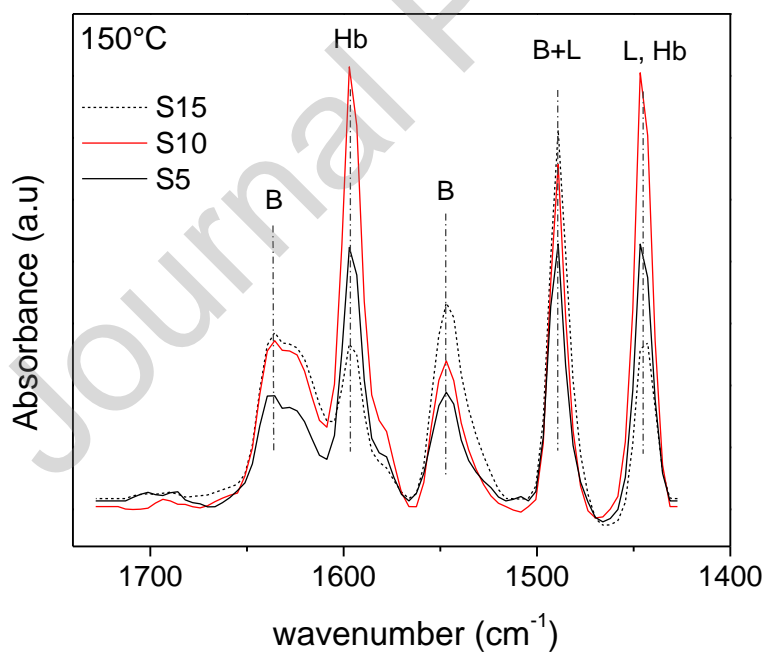


**Figure 2.** Py-FTIR of fresh propyl sulfonic SBA-15: S5, S10 and S15 samples after desorption at 150 °C. Hydrogen bond (Hb), Brønsted (B) and Lewis (L) sites.

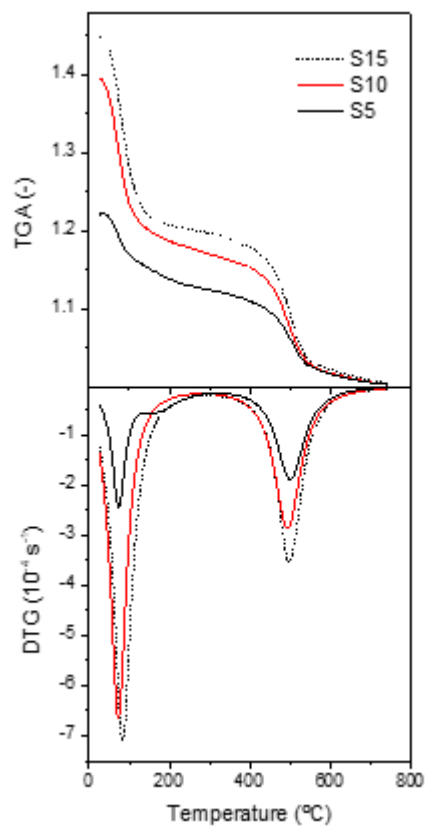


**Figure 3.** DTG profiles by TGA for the fresh propyl sulfonic SBA-15: S5, S10 and S15.

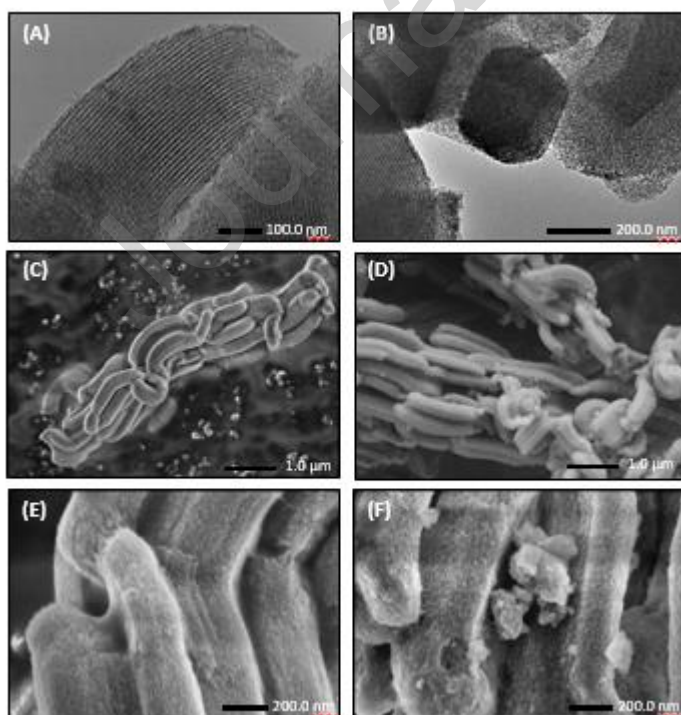


**Figure 4:** TEM images for fresh S10 (A) and S15 (B). SEM images for fresh S15 (C) and S5 (D) and fresh S15 (E) and used S15\* (F).

\* Reaction conditions: 60 °C, 2 h, 500 rpm, catalyst/FAL = 4 mg cat. (g<sub>FAL</sub>)<sup>-1</sup>, 2-MF/FAL = 2, sealed reactor.

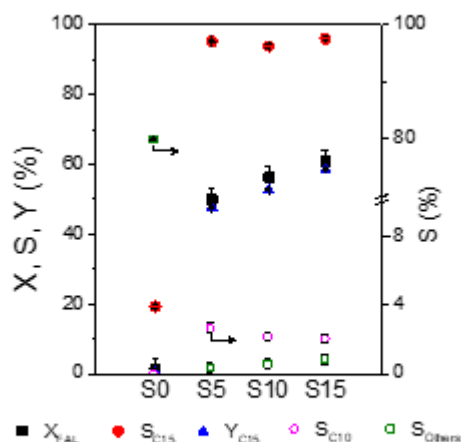


**Figure 5:** Reaction test results for S0, S5, S10 and S15 at the same conditions: 60 °C, 500 rpm, catalyst/FAL ratio = 3.2 mg cat. (g furfural)<sup>-1</sup>, 2-MF/FAL ratio = 2 (stoichiometric), 2 h, sealed reactor.  $X_{FAL}$  Conversion of furfural,  $S_{C15}$  selectivity to trimer C15,  $Y_{C15}$  yield of trimer C15,  $S_{C10}$  selectivity to dimer C10,  $S_{Others}$  selectivity to other products.

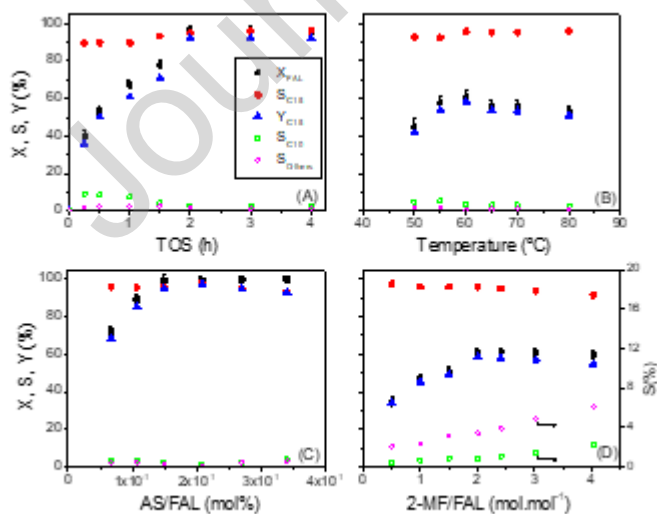


**Figure 6:** Reaction test results of catalyst S15 in sealed reactor: **(A)** Effect of the time on reaction (TOS): Conditions: 50 °C, 500 rpm, AS/FAL = 0.14 mol%, 2-MF/FAL = 2 mol.mol<sup>-1</sup>

(stoichiometric). **(B)** Effect of reaction temperature. Conditions: 500 rpm, AS/FAL = 0.037 mol%, 2-MF/FAL = 2 mol.mol<sup>-1</sup> (stoichiometric), 2 h. **(C)** Effect of AS/FAL ratio: Conditions: 50 °C, 500 rpm, 2-MF/FAL = 2 mol.mol<sup>-1</sup> (stoichiometric), 2 h **(D)** Effect of 2-MF/FAL ratio: Conditions: 60°C, 500 rpm, AS/FAL=0.037 mol%, 2 h.  $X_{FAL}$  Conversion of furfural,  $S_{C15}$  selectivity to trimer C15,  $Y_{C15}$  yield of trimer C15,  $S_{C10}$  selectivity to dimer C10,  $S_{Others}$  selectivity to others.

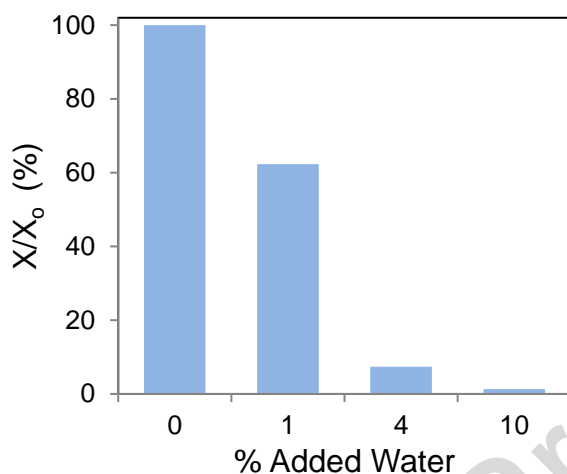


**Figure 7:** Effect of adding water to the feed for catalyst S15. Relative furfural conversion ( $X/X_0$ ) vs water percentage of the total feed. Conditions: 60 °C, 500 rpm, catalyst/FAL ratio = 3.2 mg cat. (g furfural)<sup>-1</sup>, 2-MF/FAL ratio = 2 (stoichiometric) 2 h, sealed reactor

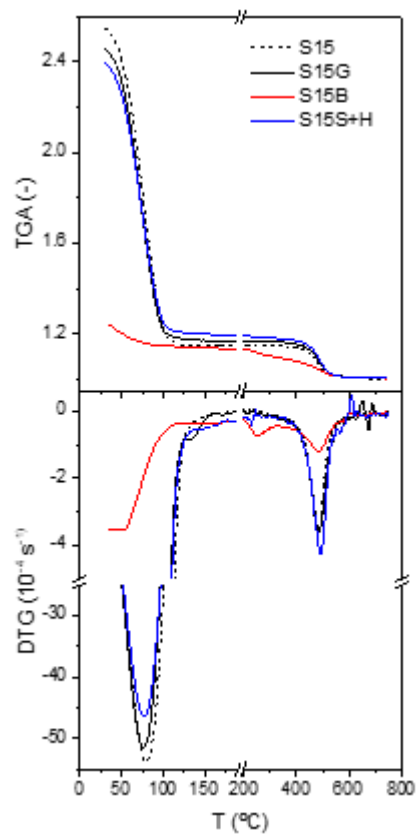


**Figure 8:** TGA and DTG profiles for fresh catalyst S15 and the hydrophobicity modified propylsulfonic SBA-15, S15S+H.

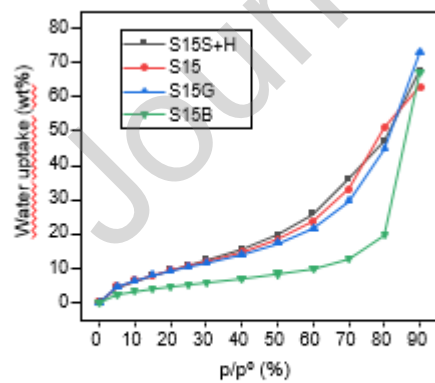


**Figure 9:** Water sorption curves for S15, S15S+H, S15G and S15B.

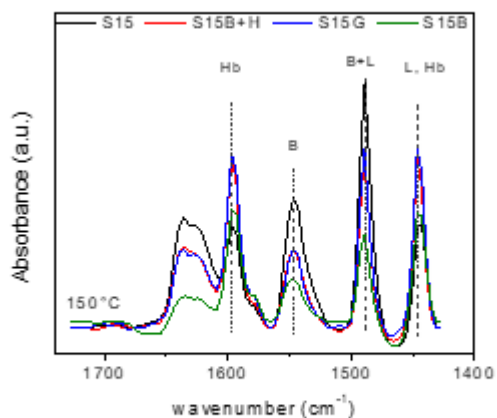


**Figure 10:** Py-FTIR of S15, S15B+H, S15G and S15B samples at 150°C with Hydrogen bond (Hb), and Bronsted (B) and Lewis (L) sites.

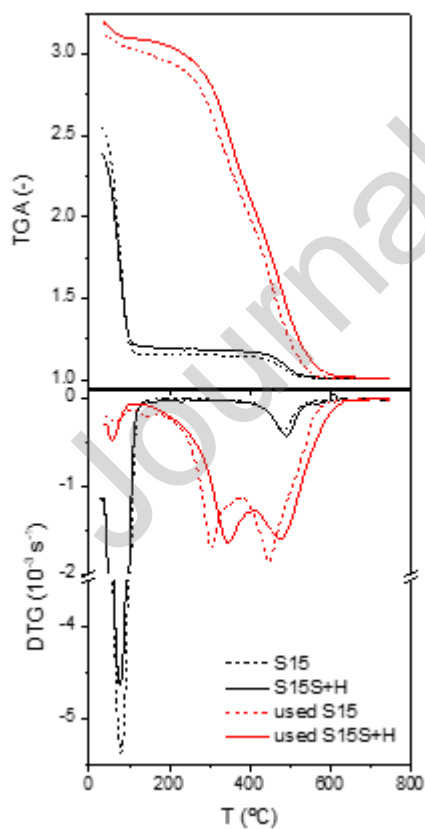


**Figure 11:** TGA and DTG profiles for fresh and used S15 and S15S+H. Reaction conditions: 60 °C, 2 h, 500 rpm, catalyst/FAL = 4 mg cat. (g<sub>FAL</sub>)<sup>-1</sup>, 2-MF/FAL = 2, sealed reactor.

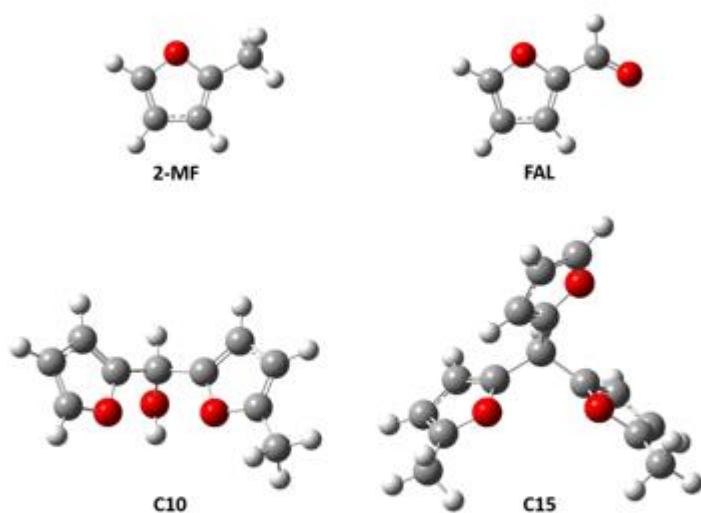


**Figure 12:** Optimized geometries of reactants and products molecules: 2-methylfuran (2-MF), furfural (FAL), monomer (C10) and dimer (C15) (O =red; C =gray; H = white).

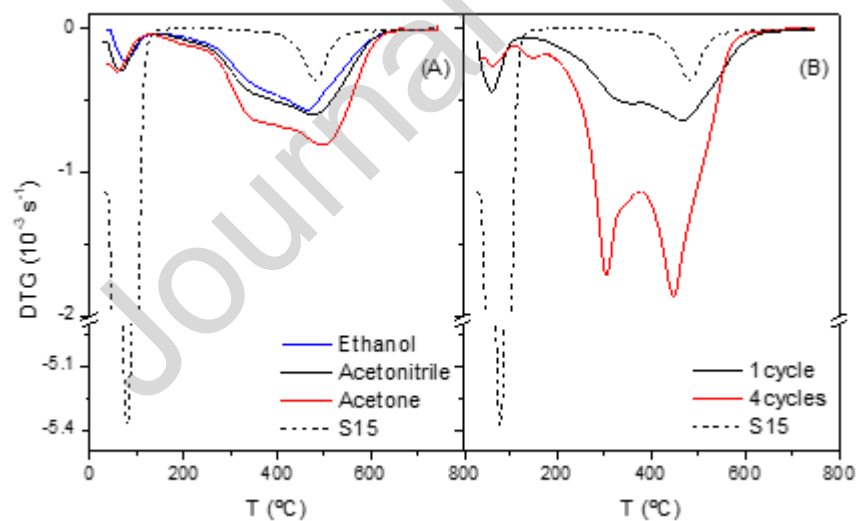


**Figure 13.** (A) DTG profiles by TGA studies of fresh and used S15 after washing with different solvents. (B) DTG profiles by TGA studies of fresh and used S15 after 1 and 4 cycles of washing with acetonitrile and reuse (Reaction conditions of Table 5).

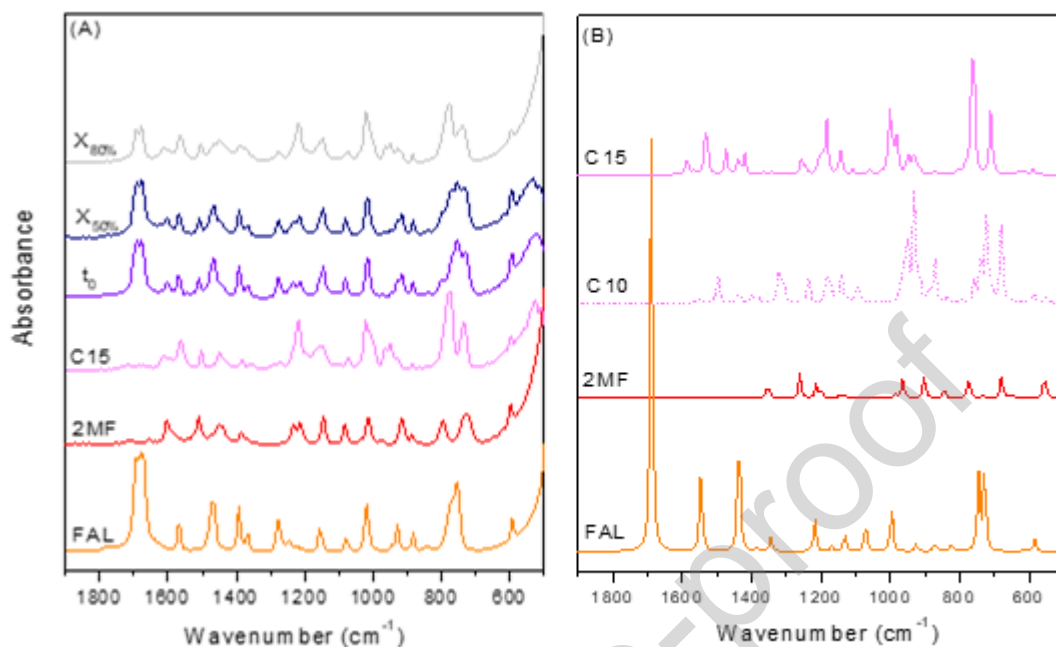


**Figure 14:** FTIR characterization of liquid phases of the reaction. A) Experimental FTIR spectra of samples; B) Theoretical FTIR of reactants and products. (FAL: furfural, 2-MF: 2-methylfuran, C15: trimer, t<sub>0</sub>: reactants mixture at t=0 min, X<sub>50%</sub>: reaction sample at 50 % of conversion of furfural, X<sub>80%</sub>: reaction sample at 80 % conversion of furfural).

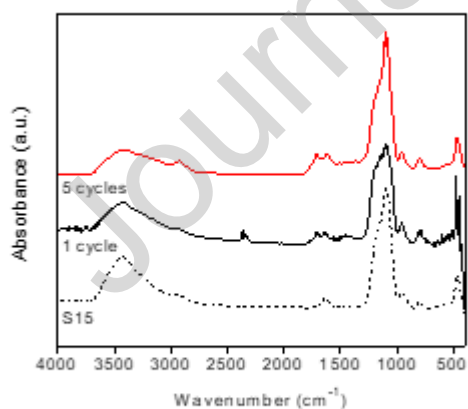


**Figure 15:** FTIR study of fresh and used S15 after 3 and 5 cycles of washing with acetonitrile and reuse (Reaction conditions of Table 5).

## Tables

**Table 1.** Characterization of S0, S5, S10 y S15.

	<b>S0</b>	<b>S5</b>	<b>S10</b>	<b>S15</b>
S/Si (mol%)	-	4	5.5	7.0
Acid sites concentration, by potentiometric titration (mmol g <sup>-1</sup> )	<0.05	0.70	0.88	1.18
BET Area (m <sup>2</sup> g <sup>-1</sup> )	627	498	632	604
Pore volume (m <sup>3</sup> g <sup>-1</sup> )	1.27	1.06	1.15	1.16
Pore diameter (nm)	10.0	10.0	10.1	10.1
Interplanar distance, d <sub>100</sub> (nm)	10.5	10.9	11.0	11.1
Lattice constant, a <sub>0</sub> (nm)	12.1	12.6	12.7	12.8
Wall thickness (nm)	2.1	2.6	2.6	2.7

**Table 2:** Hydrophobicity modified propyl sulfonic SBA-15 characterization results

	<b>S15</b>	<b>S15B</b>	<b>S15G</b>	<b>S15S+H</b>
S/Si (mol%)	7.0	2.2	7.1	7.7
Acid sites (AS) by potentiometric titration (mmol g <sup>-1</sup> )	1.12	0.46	1.05	1.11
BET area (m <sup>2</sup> g <sup>-1</sup> )	604	512	638	653
Pore Volume (m <sup>3</sup> g <sup>-1</sup> )	1.16	1.27	1.22	1.31
Pore diameter (nm)	10.1	11.5	10.0	10.0
X/Y (%)*	61/58	19/17	54/50	66/63
TON*	1543	1322	1618	1929

\*60 °C, 2 h, 500 rpm, 2-MF/FAL = 2 (stoichiometric), 0.3 mg cat.(g<sub>FAL</sub>)<sup>-1</sup>, sealed reactor.

**Table 3.** Values of molar volume and thermodynamic properties calculated by DFT

Molecule	MV (Å <sup>3</sup> )	D (Å)	E (kcal mol <sup>-1</sup> )	ΔH* (kcal mol <sup>-1</sup> )	ΔG* (kcal mol <sup>-1</sup> )
FAL	146	6.5	-215517.00	-53.71	-31.11
2-MF	113	6.0	-169064.05	-64.93	-43.04
C10	283	8.1	-384584.90	-121.11	-88.20
C15	304	8.3	-505679.42	-169.80	-129.81
H <sub>2</sub> O	28	3.7	-47971.49	-15.75	-2.31

MV=molecular volume; D=kinetic diameter; E=optimization energy; ΔH=enthalpy; ΔG=Gibb free energy; \* calculated at 50 °C.

**Table 4:** Values of molar volume and thermodynamic properties calculated by DFT

Reaction	ΔH <sub>R</sub> * (kcal/mol)	ΔG <sub>R</sub> * (kcal/mol)
2-MF + FAL → C10	-2.47	-14.05
2 2-MF + FAL → C15 + H <sub>2</sub> O	-1.97	-14.93

ΔH<sub>R</sub>=enthalpy reaction; ΔG<sub>R</sub>=Gibb free energy reaction; \* determinate at 50 °C

**Table 5:** Stability test results:

	Cycle	1	2	3	4	5
S15	X <sub>F</sub> (%)	72	69	65	15	4
	Y <sub>C15</sub> (%)	68	67	62	14	3
S15S+H	X <sub>F</sub> (%)	81	88	82	55	19
	Y <sub>C15</sub> (%)	77	83	79	53	18

60 °C, 2 h, 500 rpm, catalyst/FAL = 4 mg cat. (g<sub>FAL</sub>)<sup>-1</sup>, 2-MF/FAL = 2, sealed reactor

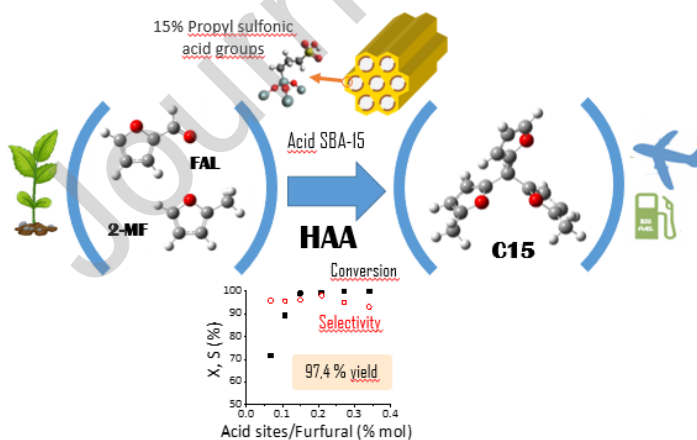
## CRedit authorship contribution statement

**M. S. Zanuttini:** Methodology, validation, investigation, formal investigation; writing original draft, funding acquisition; **C. Neyertz:** Methodology, validation, investigation, formal investigation; writing-review&edit; **L.G. Tonutti:** investigation, formal analysis, writing original draft; **C. Ferretti:** Formal analysis; Investigation; Methodology, Software, writing-review&edit; Validation; **B.O. Dalla Costa:** conceptualization, writing-review&edit; editing; **B. Sanchez:** conceptualization, methodology, writing-review&edit; editing; **A. Querini:** supervision, funding acquisition, writing-review&edit; editing,.

## Declaration of Competing Interest

The authors declare that they have no known competing financial interests or personal relationships that could have appeared to influence the work reported in this paper.

## Graphical abstract



## Highlights

- High molecular weight jet-fuel precursor synthesis from fully renewable furfural-derived reagents under mild solvent-free conditions
- Highly active modified sulfonic SBA-15 catalysts for hydroxyalkylation/alkylation C-C coupling (HAA) with yields greater than 97%.
- Great influence of concentration of Brønsted active sites on the catalytic performance.
- Strong negative influence of water in the kinetics of the reaction and in the stability of the catalysts.
- Tuning the catalysts by modifying of the hydrophobicity improved up the efficiency of the reaction.